Molecular Crystals and Liquid Crystals
Publication details, including instructions for authors and subscription information:
http://www.tandfonline.com/loi/gmcl20

# Electric Field Induced Biaxial Order and Differential Quenching of Uniaxial Fluctuations in a Nematic with Negative Dielectric Anisotropy

Volodymyr Borshch [a], Sergij V. Shiyanovskii [a] & Oleg D. Lavrentovich [a]

[a] Liquid Crystal Institute and Chemical Physics Interdisciplinary Program, Kent State University, Kent, USA

Version of record first published: 11 May 2012.

To cite this article: Volodymyr Borshch , Sergij V. Shiyanovskii & Oleg D. Lavrentovich (2012): Electric Field Induced Biaxial Order and Differential Quenching of Uniaxial Fluctuations in a Nematic with Negative Dielectric Anisotropy, Molecular Crystals and Liquid Crystals, 559:1, 97-105

To link to this article: http://dx.doi.org/10.1080/15421406.2012.658691

*Mol. Cryst. Liq. Cryst.*, Vol. 559: pp. 97–105, 2012

ISSN: 1542-1406 print/1563-5287 online
DOI: 10.1080/15421406.2012.658691

Taylor & Francis
Taylor & Francis Group

# Electric Field Induced Biaxial Order and Differential Quenching of Uniaxial Fluctuations in a Nematic with Negative Dielectric Anisotropy

VOLODYMYR BORSHCH, SERGIJ V. SHIYANOVSKII,* AND OLEG D. LAVRENTOVICH

Liquid Crystal Institute and Chemical Physics Interdisciplinary Program, Kent State University, Kent, USA



*We explore the response of a uniaxial nematic liquid crystal with a negative dielectric anisotropy to the electric field applied normally to the director. The geometry causes two effects: field-induced biaxiality order (FIBO) and differential quenching of uniaxial fluctuations (DQUF). We separate the two effects by tracing the field-induced changes in optical response at the timescales of nanoseconds. The study paves the way to establish the possibility of field-assisted formation of the biaxial nematic phase and to explore the likelihood of the appearance of biaxial order in the field-free conditions.*

**Keywords** Dynamics; field-induced biaxiality; fluctuations; nematic liquid crystal

## 1. Introduction

An electric field applied to a dielectric can change the structural symmetry and thus the optical properties of the material. If the material is isotropic, the electric field can induce an optically anisotropic uniaxial state; the effect is well known as the Kerr effect. If the isotropic dielectric represents a melted state of a liquid crystal (LC), then the Kerr effect becomes more pronounced as the temperature is reduced towards the transition point into the LC. When the material is already in the nematic LC state, the most evident effect of the applied electric field is reorientation of the optic axis (the director) either along the field (if the dielectric anisotropy is positive) or perpendicular to the field if the dielectric anisotropy is negative. Of especial interest is the situation when the electric field does not cause macroscopic director reorientation of the uniaxial nematic LCs [1–4], for example, when the electric field is applied perpendicularly to the director $\hat{\mathbf{n}}$ of a LC with negative dielectric anisotropy, $\Delta\varepsilon = \varepsilon_{\parallel} - \varepsilon_{\perp} < 0$. In this case, the applied electric field can change the overall symmetry of the LC, inducing a secondary axis of molecular order that is perpendicular to $\hat{\mathbf{n}}$ so that the material in the field becomes a biaxial nematic [5]. This effect can be called field-induced biaxial order (FIBO). Development of bent-core LC materials and an intensive search for the biaxial nematic phase lead to a renewed interest to FIBO [6–8]. The challenge in characterizing the possible FIBO is that the field can also modify the fluctuations of the main (uniaxial) director $\hat{\mathbf{n}}$ [1,9–13]. These changes in fluctuations

*Address correspondence to Sergij Shiyanovskii, Liquid Crystal Institute and Chemical Physics Interdisciplinary Program, Kent State University, Kent, OH 44242, USA. Tel: +1 (330) 672-1576; Fax: +1 (330) 672-2796. E-mail: sshiyano@kent.edu

of $\hat{\mathbf{n}}$ are anisotropic. Imagine, for example, a planar LC slab cell with $\hat{\mathbf{n}} = (1, 0, 0)$ and $\Delta\varepsilon = \varepsilon_{\parallel} - \varepsilon_{\perp} < 0$ under the action of the applied electric field, $\mathbf{E} = (0, 0, E)$. The applied electric field supresses the fluctuations of $\hat{\mathbf{n}}$ in the vertical $(x,z)$ plane but hardly affects the fluctuations in the horizontal $(x,y)$ plane. The effect can be called a 'differential quenching of uniaxial fluctuations' (DQUF) [12a]. Dunmur and Palffy-Muhoray [14] provided a theoretical description of how the FIBO and DQUF effects modify the optical properties of a uniaxial nematic.

Experimental separation of FIBO from DQUF represents a formidable challenge, as qualitatively described below. The DQUF induces changes of the effective birefringence of the sample that are linearly proportional to the amplitude of the applied field (page 148 of [1]), $\delta\Delta n \propto |E|$. The field-induced change in the effective birefringence measured in the $(x,y)$ plane and caused by FIBO effect, should be quadratic in the applied field ($\delta\Delta n \propto E^2$), thanks to the nonpolar character of the nematic and molecular dielectric biaxiality (individual molecules are not axially symmetric). One thus expects the DQUF effect to dominate FIBO at relatively low fields. To separate the two, we propose to use the difference in characteristic relaxation times. The FIBO effect is expected to be fast, because it results from molecular orientational order. For example, the field-induced changes in the uniaxial scalar order parameter occur at the timescale of less than 100 ns [15]. On the other hand, the DQUF is expected to be slower, as described by the field-induced director reorientation with characteristic time $\tau_f^{ON} \sim \gamma/(|\Delta\varepsilon|\,\varepsilon_0 E^2)$, which results in an estimate $\tau_f^{ON} \sim 20\,\mu$s for $E = 10^7\,\mathrm{V\,m^{-1}}$, with the typical values of the rotational viscosity $\gamma = 0.1\,\mathrm{Pa \cdot s}$, and dielectric anisotropy $\Delta\varepsilon = -6$.

In this work, we explore the nanosecond dynamics of field-induced optical birefringence changes in a dielectrically negative uniaxial nematic, with the goal of experimental separation of FIBO and DQUF. Section 2 describes the experiments. Section 3 presents the theoretical model. Section 4 discusses the results.

## 2. Experimental Technique

We use a single component nematic 4′-butyl-4-heptyl-bicyclohexyl-4-carbonitrile (abbreviated as CCN-47) provided by Nematel GmbH (Fig. 1), with negative dielectric anisotropy $\Delta\varepsilon = -6$. CCN-47 is filled into a planar cell of a thickness $d = 7.9\,\mu$m. The inner surfaces of the cell's bounding plates are coated with a polyimide layer PI-2555 (Nissan Chemicals) and rubbed in the antiparallel directions. All the measurements were performed in the nematic phase of the material at 35°C. The temperature is stabilized by Linkam LTS350 hotstage.

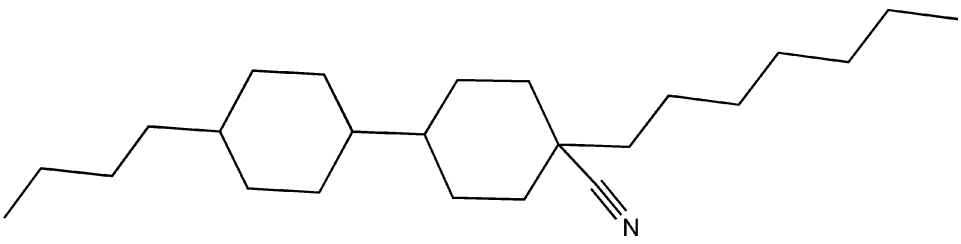


**Figure 1.** Structure of a molecule of CCN-47. Negative dielectric anisotropy is due to the transverse cyano-group dipole. The other name is ZLI-2705. CAS number 102714-85-2.

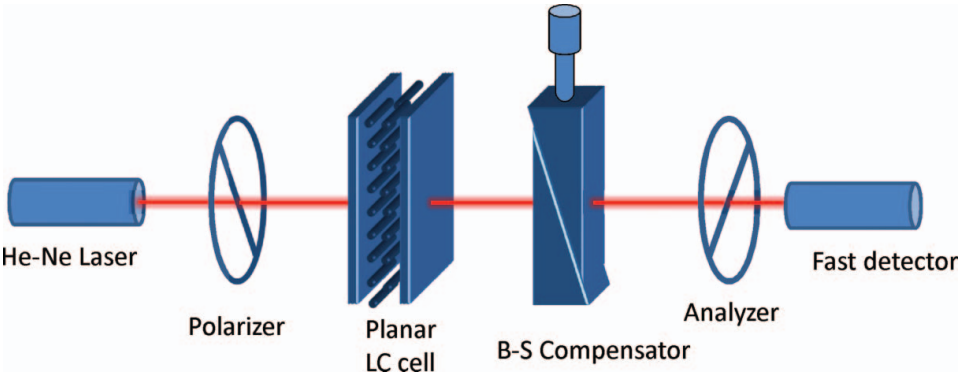


**Figure 2.** The experimental setup. Adding additional phase difference of $\pi/2$ by the Babinet-Soleil compensator (B-S) allows to separate optical phase retardation part of the signal from other effects (change of light scattering or other parasitic effects).

The field induced birefringence dynamics is monitored by measuring the intensity $I = I_0 \sin^2 \frac{\pi L}{\lambda}$ ($L = \Delta n d$ is the retardance, $\Delta n$ is the effective birefringence, and $d$ is the cell thickness) of laser beam (He-Ne, $\lambda = 633$ nm) passing through the cell and two crossed linear polarizers (Fig. 2). The rubbing direction of the cell is at 45° with respect to the polarizers. The Babinet-Soleil compensator introduces a controllable retardance, that is chosen to set the linear regime in which $\Delta I \propto \Delta L$ ($L \approx (k+1/2)\lambda$, $k$ integer), where small changes in retardance lead to pronounced modulation of the transmitted light intensity.

Because we trace the dynamics of optical changes at the scale of nanoseconds, it is important to keep the *RC* delay time of the cell as small as possible. Small *RC* time ensures short time of charging the cell, thus minimizing the delay time when the electric field is applied to the LC inside this cell. For this purpose we use low-resistance ITO electrodes (10 Ω/square) and make the electrode area small (around 2 mm$^2$). The measured capacitance of the cell filled with CCN-47 is 41 pF at 35°C. Applying a rectangular pulse and measuring the current through the cell, we confirm that *RC* time is about 1–2 ns.

The driving voltage pulse with a sharp front (5 ns rise time) is produced by a generator DEI HV1000 (Direct Energy). Voltage pulses of different amplitude and of duration $t_p = 1.177\,\mu$s are applied to the LC cell, and the optical response is measured using a fast photodetector TIA-500S-TS (Terahertz Technologies) with the response time $<1$ ns (Fig. 3). The voltage pulses and photodetector signals are measured with 1 GS/s digital oscilloscope TDS2014 (Tektronix).

Because the rise time of the voltage pulses and the RC-time of the cell are short as compared to the relaxation times of the optical response, the front and back edges of the voltage pulses are considered to be instantaneous. The voltage amplitude achieved immediately after the front edge, however, is not a constant and shows a slow decrease with time. This slow decrease is well modelled by the function $U(t) = U_0 e^{-\nu t}$, where $U_0$ and $\nu$ are the fitting parameters (Fig. 3(a)). The time dependence of the electric field $E(t) = U(t)/d$ is then:

$$E(t) = \frac{U_0}{d} e^{-\nu t}. \tag{1}$$

Figure 3b represents the main experimental result of this work. It shows the dynamics of an increase (field ON) and decrease (field OFF) of the field-induced optical retardance

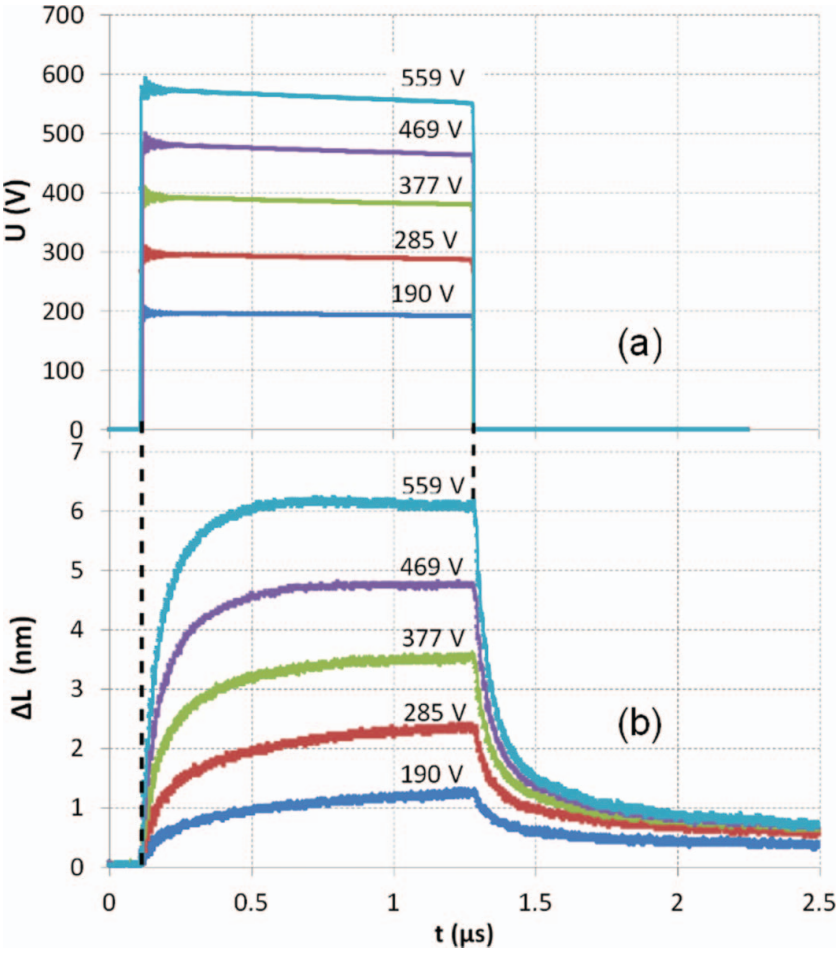


**Figure 3.** Typical voltage pulses (a) applied to the CCN-47 cell, and the corresponding optical responses (b) as detected by the fast photodetector.

for five different amplitudes of voltage applied to the CCN-47 cell. Below we present our model to fit this dynamics and to separate the contributions of FIBO and DQUF.

## 3. Model

To analyse the experimental data we consider the total change of the retardance, caused by the applied electric field, $\Delta L(t) = L(t) - L(0) = \Delta L_b(t) + \Delta L_f(t)$, as a sum of the contributions from FIBO effect, $\Delta L_b(t)$, and DQUF effect, $\Delta L_f(t)$. Both effects are small, thus we can neglect the terms describing the coupling of these two.

We assume that the dynamics of the system is controlled by the linear response and ascribe a single relaxation time $\tau_b$ to the FIBO process:

$$\tau_b \frac{d\Delta L_b(t)}{dt} = \Delta \bar{L}_b(t) - \Delta L_b(t), \tag{2}$$

where $\Delta\bar{L}_b(t) = c_b E^2(t)d$ is an equilibrium contribution corresponding to the instantaneous value of the electric field $E(t)$ at the moment of time $t$ and $c_b$ is the susceptibility parameter of the LC. The solution of Eq. (2), when $E(t)$ turns on at $t = 0$, is

$$\Delta L_b(t) = \int_0^t \frac{\Delta\bar{L}_b(t')}{\tau_b} e^{-(t-t')/\tau_b} dt'. \tag{3}$$

Substituting (1) in (3), we obtain the solutions for the ON and OFF processes:

$$\Delta L_b^{ON}(0 < t \le t_p) = \frac{c_b U_0^2}{d(1 - 2\nu\tau_b)}(e^{-2\nu t} - e^{-t/\tau_b}) \quad \text{and} \tag{4}$$

$$\Delta L_b^{OFF}(t > t_p) = \Delta L_b^{ON}(t_p)\exp(-(t - t_p)/\tau_b), \tag{5}$$

where $t_p$ is the duration of the applied voltage pulse.

The analysis of $\Delta L_f(t)$ is more complicated because $\Delta L_f(t) = \sum_{\mathbf{q}} \Delta L_f(\mathbf{q}, t)$ contains contributions from the entire spectrum of fluctuations with different wavevectors $\mathbf{q}$. We describe each $\Delta L_f(\mathbf{q}, t)$ by a linear response equation, similar to (2):

$$\tau(\mathbf{q}, t)\frac{d\Delta L_f(\mathbf{q}, t)}{dt} = \Delta\bar{L}_f(\mathbf{q}, t) - \Delta L_f(\mathbf{q}, t), \tag{6}$$

where the relaxation time $\tau(\mathbf{q}, t)$ and quasi-equilibrium value $\Delta\bar{L}_f(\mathbf{q}, t)$ depend on $\mathbf{q}$ and current field $E(t)$. In one-constant approximation for the elastic moduli, $K_{11} = K_{22} = K_{33} = K$,

$$\tau(\mathbf{q}, t) = \frac{\gamma_{eff}}{Kq^2 + |\Delta\varepsilon|\,\varepsilon_0 E^2(t)}, \qquad \Delta\bar{L}_f(\mathbf{q}, t) \propto \frac{|\Delta\varepsilon|\,\varepsilon_0 E^2(t)}{Kq^2(Kq^2 + |\Delta\varepsilon|\,\varepsilon_0 E^2(t))}, \tag{7}$$

where $\gamma_{eff}$ is the effective rotational viscosity and $\varepsilon_0$ is the dielectric permittivity of free space.

During the ON process, the main contribution to the optical phase retardation is provided by the fluctuations with $q < q_E = E\sqrt{|\Delta\varepsilon|\,\varepsilon_0/K}$ (for $E \sim 10^7\,\mathrm{V\,m^{-1}}$, $q_E \sim 10^7\,\mathrm{m^{-1}}$), that have approximately the same characteristic time

$$\tau_f^{ON} = \gamma_{eff} d^2/|\Delta\varepsilon|\,\varepsilon_0 U_0^2. \tag{8}$$

Thus for the ON process of DQUF, one may write an equation similar to (2):

$$\tau_f^{ON}\frac{d\Delta L_f^{ON}(t)}{dt} = \Delta\bar{L}_f(t) - \Delta L_f^{ON}(t), \tag{9}$$

where $\Delta\bar{L}_f(t) = \sum_{\mathbf{q}} \Delta\bar{L}_f(\mathbf{q}, t) = c_f|E(t)|\,d$ [7], and $c_f$ is the LC material parameter. Using (1), we find a solution of Eq. (9):

$$\Delta L_f^{ON}(0 < t \le t_p) = \frac{c_f U_0}{1 - \nu\tau_f^{ON}}\left(e^{-\nu t} - e^{-t/\tau_f^{ON}}\right). \tag{10}$$

To model $\Delta L_f^{OFF}(t > t_p)$, when the electric field is turned off and each fluctuation relaxes with its own characteristic time $\tau(q) = \gamma/Kq^2$, we split the fluctuations into two

types: 'fast' fluctuations described by phenomenological relaxation time $\tau_f^{OFF}$, and 'slow' ones that provide a constant contribution during the time of experiment (several microseconds):

$$\Delta L_f^{OFF}(t > t_p) = \Delta L_f^{ON}(t_p)\left[(1 - r_0)\exp\left(-(t - t_p)/\tau_f^{OFF}\right) + r_0\right], \tag{11}$$

where $r_0$ is the relative contribution of slow fluctuations.

To summarize our model, $\Delta L(t) = \Delta L_b(t) + \Delta L_f(t)$ is described by equations (4), (5), (10), and (11), with six fitting parameters: material parameters $c_b$, $c_f$, relaxation times $\tau_b$, $\tau_f^{ON}$, and $\tau_f^{OFF}$, and the relative contribution of slow fluctuations $r_0$. The parameters $U_0$ and $\nu$ are found from the independent fitting of the voltage pulse with (1).

## 4. Results and Discussion

Figure 4 shows how the experimental data on dynamics of optical response are fitted with the model for a pulse with $U_0 = 557$ V. The functions describing FIBO by Equations (4), (5) and DQUB by (10), (11) fit the data well, never deviating beyond the experimental noise. The fitting parameters for this voltage pulse are: $\tau_b = 44$ ns, $\tau_f^{ON} = 194$ ns, $\tau_f^{OFF} = 292$ ns, $r_0 = 0.31$, $c_b = 5.1 \times 10^{-13}\,\mathrm{m^2V^{-2}}$, $c_f = 2.1 \times 10^{-5}\,\mathrm{m\,V^{-1}}$. Based on these values, we separate FIBO (dotted line on Fig. 4) and DQUF components of the optical response. The same approach is used in analysing the data for other voltages.

The fitting of the experimental data supports the basic predictions of the model Figs 5, 6. First, the susceptibility parameters $c_b$ and $c_f$ are practically voltage-independent, Fig. 5. Second, the biaxial time $\tau_b$ does not depend on the electric field, Fig. 6. We performed an additional fitting with two independent values of $\tau_b$, one for the ON branch, Eq. (4), and another for the OFF branch, Eq. (5). This fitting resulted in two values of $\tau_b$ that

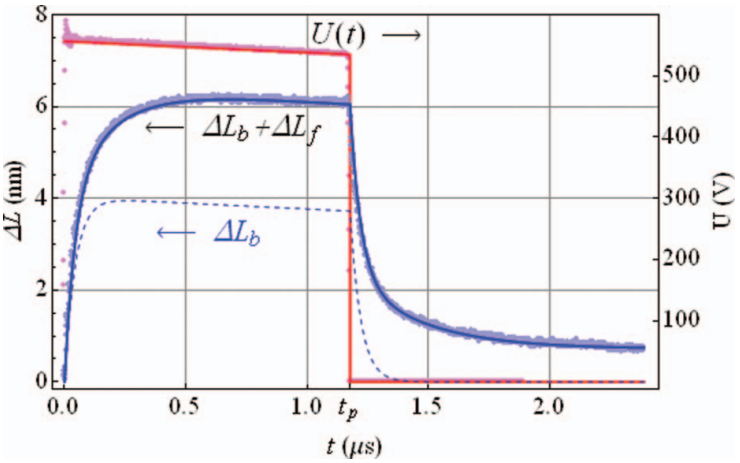


**Figure 4.** The experimental points of the optical response (light blue dots) are fitted with the equations (4), (5) (rising blue line), and (10), (11) (decaying blue line). The fitting parameters are: $\tau_b = 44$ ns, $\tau_f^{ON} = 194$ ns, $\tau_f^{OFF} = 292$ ns, $r_0 = 0.31$, $c_b = 5.1 \times 10^{-13}\,\mathrm{m^2V^{-2}}$, $c_f = 2.1 \times 10^{-5}\,\mathrm{m\,V^{-1}}$. The dashed blue line corresponds to BIF component of the optical retardance expressions (4) and (5). The pink dots are the experimental measurement of the applied voltage described by equation (1) (red line) with fitting parameters $U_0 = 557$ V and $\nu = 34 \times 10^3\,\mathrm{s^{-1}}$.

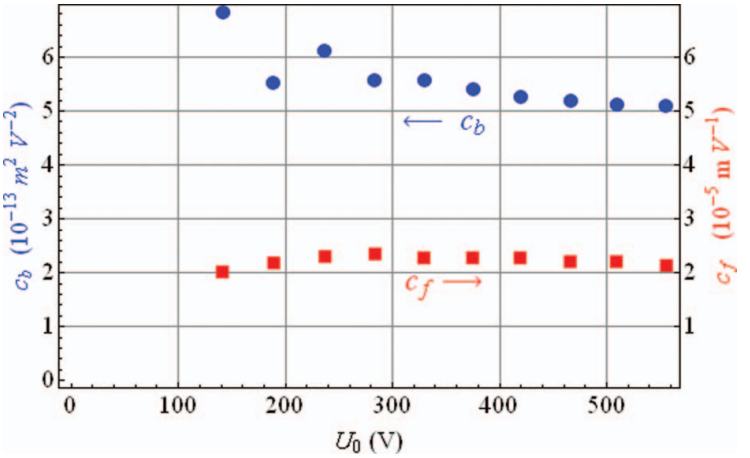


**Figure 5.** The dependence of the biaxial $c_b$ (blue circles) and fluctuational $c_f$ (red squares) susceptibilities on the maximum applied voltage $U_0$. According to our model they should not depend on the applied electric field.

differ by less than 10%, supporting the idea that $\tau_b$ is a single parameter for both processes. Third, $\tau_f^{ON}$ decreases at higher voltages. The model, Eq. (8), does predict such a decrease, but with a rate $\tau_f^{ON} \sim U^{-2}$ that is somewhat higher than the experimental trend $\tau_f^{ON} \sim U^{-1}$. The reason for this discrepancy is rooted in the fact that the model approximates the collective behaviour of all fluctuations with a single time constant and thus anticipates a steeper voltage dependency. Finally, note that the phenomenological time constant $\tau_f^{OFF}$ and the relative contribution $r_0$ of the slow fluctuations in DQUF show a weak decrease with the applied voltage, Figs 6, 7.

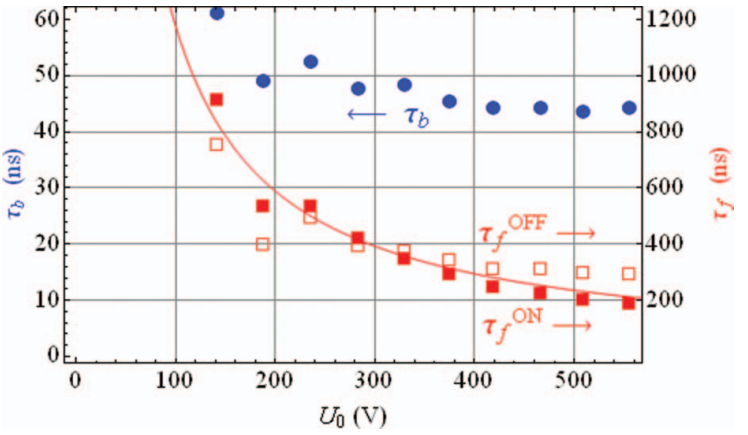


**Figure 6.** The dependence of the characteristic times $\tau_b$ (solid blue circles), $\tau_f^{ON}$ (solid red rectangulars), and $\tau_f^{OFF}$ (open red rectangulars) on the maximum applied voltage $U_0$. According to our model the biaxial time $\tau_b$ has to be constant. The behaviour of $\tau_f^{OFF}$ fits well with $U_0^{-1}$ function (red curve).

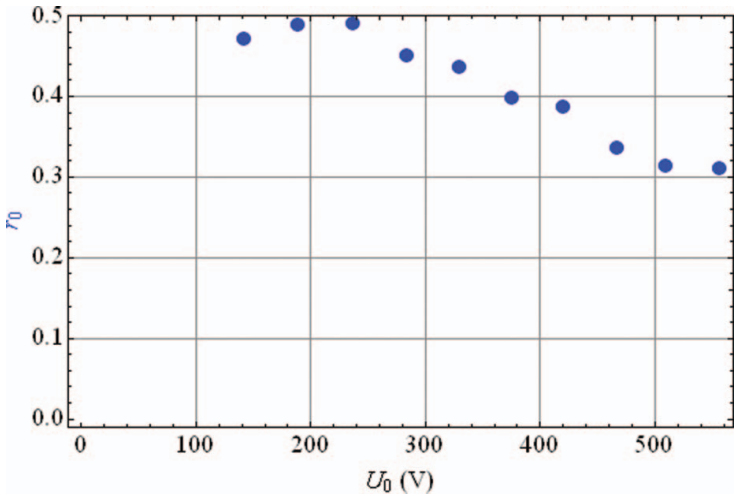


**Figure 7.** The dependence of relative amplitude $r_0$ of the slow fluctuations on the maximum applied voltage $U_0$.

The pulse duration $t_p$, slightly higher than 1 $\mu$s, turns out to be sufficiently large as compared to the time constants found from the fitting of data. Therefore, the experimentally measured optical retardance at the end of the applied pulse should be close to the values that correspond to the stationary values (under the constant electric field), for both FIBO and DQUF. We use the fitting parameters to calculate the values of $\Delta L_b^{ON}(t_p)$ and $\Delta L_f^{ON}(t_p)$ at the end of the applied pulse and to extract their dependence on the applied voltage, Fig. 8. As expected, the FIBO contribution is quadratic in the field, while the DQUF contribution is linear with the field, Fig. 8.

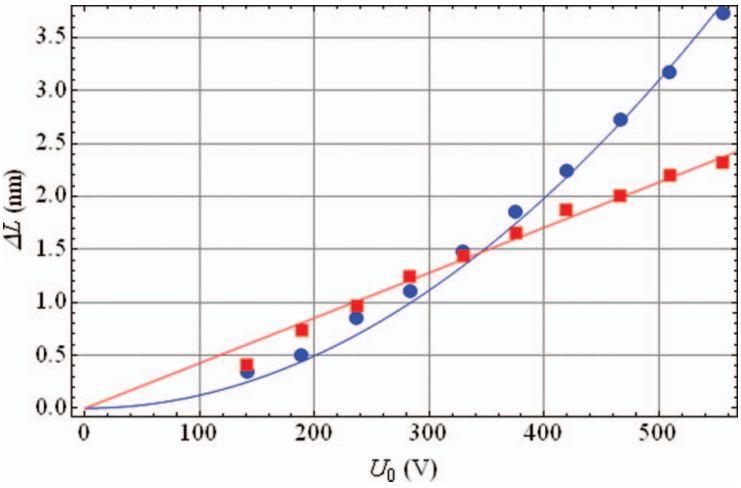


**Figure 8.** Reconstructed FIBO (obtained from Eq. (10)) and DQUF (Eq. (4)) components of retardance at time $t_p$ as function of the maximum applied voltage $U_0$.

## Conclusions

We have explored the response of a uniaxial nematic liquid crystal with a negative dielectric anisotropy to the electric field applied normally to the director. We used the idea of different relaxation times to separate the effects associated with the field-induced biaxial order (FIBO) and with differential quenching of uniaxial fluctuations (DQUF). The experimental data suggest that the dynamics of optical response does indeed allows one to extract the effect of FIBO at the background of DQUF despite the fact that the studied material CCN-47 shows no signs of the biaxial nematic order in the field-free state. This approach will be used in further studies of field-induced biaxial order in uniaxial nematic liquid crystals as well as in the search of the materials in which the biaxial nematic order can appear even without the applied field.



## Acknowledgments

This work was supported by DOE Grant #DE-FG02-06ER 46331. The authors thank R. Eidenschink (Nematel GmbH) for providing us with CCN-47 for the experiment.

## References

[1] de Gennes, P. G., & Prost, J. (1995). *The Physics of Liquid Crystals,* 2nd edition, Oxford University Press: Oxford.
[2] Fan, Ch.-P., & Stephen, M. J. (1970). *Phys. Rev. Lett.*, *25*, 500.
[3] Lelidis, I., & Durand, G. (1998). In: P. E. Cladis & P. Palffy-Muhoray (Eds.), *Dynamics and Defects in Liquid Crystals, Chapter 'Thermal Entropic Effect at the Electric Field Induced Isotropic-Nematic Transition'*, Gordon and Breach Science Publishers: Amsterdam, p. 61.
[4] Lelidis, I., Nobili, M., & Durand, G. (1993). *Phys. Rev. E*, *48*, 3818.
[5] (a) Palffy-Muhoray, P., & Dunmur, D. A. (1982). *Phys. Lett.*, *91A*, 121; (b) Palffy-Muhoray, P., & Dunmur, D. A. (1983). *Mol. Cryst. Liq. Cryst.*, *97*, 337.
[6] Olivares, J. A., Stojadinovic, S., Dingemans, T., Sprunt, S., & Jákli, A. (2003). *Phys. Rev. E*, *68*, 041704.
[7] Mamatha Nagaraj, Panarin, Y. P., Manna, U., Vij, J. K., Keith, C., & Tschierske, C. (2010). *Appl. Phys. Lett.*, *96*, 0111106.
[8] Stannarius, R., Eremin, A., Tamba, M.-G., Pelzl, G., & Weissflog, W. (2007). *Phys. Rev. E*, *76*, 061704.
[9] de Gennes, P. G. (1968). *C.R. Acad. Sci., Paris*, *266B*, 15.
[10] Poggi, Y., & Filippini, J. C. (1977). *Phys. Rev. Lett.*, *39*, 150.
[11] Dunmur, D. A., Waterworth, T. F., & Palffy-Muhoray, P. (1985). *Mol. Cryst. Liq. Cryst.*, *124*, 73.
[12] (a) Dunmur, D. A., Szumilin, K., & Waterworth, T. F. (1987). *Mol. Cryst. Liq. Cryst.*, *149*, 385; (b) Dunmur, D. A., & Szumilin, K. (1989). *Liq. Cryst.*, *6*, 449.
[13] Martinand, J. L., & Durand, G. (1972). *Solid State Comm.*, *10*, 815.
[14] Dunmur, D. A., & Palffy-Muhoray, P. (1988). *J. Phys. Chem.*, *92*, 1406.
[15] Gu, M., Shiyanovskii, S. V., & Lavrentovich, O. D. (2008). *Phys. Rev. E*, *78*, 040702(R).